Electrochemical, structural, optical, and morphological characteristics of Cu-loaded ZnO nanostructures synthesized from bio-waste (maize) using a green synthesis technique

R. Jagadeeswari[a,*], G. Rathika[b], K. V. Satheesh Kumar[c], P. Selvakumar [d]
[a]*Department of Chemistry, KPR Institute of Engineering and Technology, Coimbatore -641407, India*
[b]*Department of Chemistry, PSG College of Arts & Science, Coimbatore -641014, Tamilnadu, India*
[c]*Department of Mechanical Engineering, Kongu Engineering College, Perundurai 638060, Tamilnadu, India*
[d]*Department of Chemistry, Erode Sengunthar Engineering College, Thudupathi-638057, Tamilnadu, India*

The study reports feasibility to synthesis copper loaded ZnO nanoparticles using a green synthesis approach influenced by natural extracts from waste maize materials is explored. Different methods were used to investigate the physicochemical characteristics of Cu-ZnO nanoparticles. X-ray diffraction (XRD) and Fourier transform infrared spectroscopy (FT-IR) studies were used to investigate the structural behavior of Cu-ZnO nanoparticles. XRD analysis shows that Cu-ZnO has a typical crystallite size of 23.5nm and a confirmed hexagonal structure. In the wavenumber range 400–600 cm^{-1}, FT-IR confirmed the presence of metallic elements in Cu-ZnO samples. Through the use of UV–vis spectroscopy, we were able to investigate the optical characteristics of Cu-ZnO. The samples' surface morphology was recorded by FESEM, and their elemental content was evaluated by EDX. This verifies the spherical shape of prepared samples with homogeneous size distributions across their structures. The nanostructured redox behaviour of electroactive Cu-ZnO has been investigated by cyclic voltammetry.

(Received December 19, 2022; Accepted February 27, 2023)

Keywords: Green synthesis of Cu-ZnO, Maize waste, Optical, Electrochemical properties

1. Introduction

Metal oxide nanoparticles have gained a lot of attention as a potential efficient photocatalyst during the last several decades. The transition metal oxides stand out among the other metal oxides because of the unusual features made possible by their outer d electrons[1]. Because of this, they may exhibit a broad variety of electrical and magnetic characteristics useful in many contexts. Because their physical, chemical, and biological features may be tuned to increase performance over their bulk counterpart, nano structured materials have gained prominence in technological applications with a size of at least 1-100 nm[2]. To synthesize nanomaterials, one might start from the bottom up or the top down. Top-down techniques, like pounding, involve breaking down a substance into nanoparticles. As part of the bottom-up strategy, nanomaterials are synthesized from smaller molecules. Pyrolysis (laser and spray), sol-gel, chemical vapor and bath deposition and many more chemical and physical processes are employed[3]. However, these procedures call for the employment of environmentally hazardous chemicals and solvents. Second, the extremely high-temperatures and pressures needed by several of the processes make them exceedingly energy-intensive. Furthermore, the reaction circumstances like pH, concentration, temperature, etc. affect the materials morphological aspects[4].

As a result, there are a number of obstacles that must be overcome before the materials can be put to practical use, including their instability in unfavorable environments, a lack of

* Corresponding author: jagadeeswarichem@gmail.com
https://doi.org/10.15251/DJNB.2023.181.291

knowledge of the underlying process, and a range in cost[5]. For these reasons, adapting these techniques for other purposes is challenging. There has been an explosion of interest in green chemistry synthesis in recent years due to the many benefits it has over more conventional chemical and physical processes. Biodegradable wastes are put to use as catalysts in this process, which involves the bio-oxidation and bio-reduction of a number of metal salts[6]. This technique is analogous to reduction operations(chemical) whereby the natural extracts of plants are used as reducing agents and it is used in a "bottom up" fashion to synthesize nanomaterials. Since the chemical compounds and organic solvents used in synthesis may be toxic and waste disposal is a hassle, the green synthesis method aims to reduce the potential for contamination from the outset and prevent waste from being produced in the first place[7].

Maize, often known as maize (zea mays L.), is among the most popular and widely consumed staple nutrients because to its high nutritional value and practicality as a source of energy[8]. Maize, or Zea mays, is a grass (Poaceae). When the female flowers develop into the edible ear cobs, the male flowers will have finished their job at the primary centre line of the stalk[9]. Silk, a substance similar to cotton, is used to encase the ears; its thickness increases dramatically at the ear's tip. Numerous research has shown that the zea mays lea plant, from which silk is produced, consists of the following: phytochemicals, and silk is formed from the plant's stigmas and styles. Flavonoids, proteins, steroids, phenols, carbohydrates, glycosides, terpenoids, tannins, alkaloids, vitamins, mineral elements, and a plethora of other chemical compounds are all examples of phytochemicals[10]. Although there are several reports available for the creation of metal oxide nanoparticles such as ZnO, PbS, TiO_2, CuO, Ag, etc.,[11–15] from maize waste, only small number of reports available for doping of metal oxides.

Here, we detail the synthesis of copper-doped ZnO from corn byproducts, along with its structural, optical, electrochemical, and morphological characteristics. Many of the phytochemicals in corn byproducts are effective in neutralizing the metal salts that are present. They aid in characterizing the crystalline structure, shape, and size of the produced copper doped ZnO nanoparticles.

2. Methods and materials characterization

2.1. Preparation of maize waste extract

Corn on the cob, complete with the grains and the husk, was purchased from a vendor in a local market in Coimbatore, Tamilnadu, India. After proper operation, around 50 g of raw broken husk was washed thoroughly with deionised water. Then, for about 3 hours, they were heated to 60^0C in 180 cc of purified water. An extract of pale yellow colour and pH around 4 was obtained. Drying the corn husk at 40^0C and then grinding it into a powder is how this process began. Two hours of heating 20 grams of powdered dry maize husk in 200 mL of distilled water at 60^0C yielded an extract. After heating 10 grams of maize fresh silk in 200 mL of deionised water at 60 ^{0}C for three hours, the resulting extract was collected. To prepare the extracts for use in synthesis, they were mixed and chilled to room temperature, then sieved twice through Whatman filter paper.

2.2. Synthesis of copper loaded ZnO from extract

Cu-ZnO nanoparticles were synthesized using an aqueous solution of freshly extracted maize. Using magnetic stirring, a homogenous solution of zinc nitrate (0.9 M) and copper nitrate (0.1 M) in water was created. The stock solution of 20 mL of maize extract was added dropwise in sequence to the combination of metal salts, and stirring was kept up for two hours at a temperature of 60^0C [16]. After removing the precipitate out from mixture, it was cleaned repeatedly with ethanol and purified water to get rid of any unreacted precursors. After collecting the powder, it was annealed at 400 degrees Celsius for three hours in a muffle furnace.

2.3. Characterization

Thermo Nicolet iS50, KBr pellets were employed in an FTIR spectrophotometer to analyses the vibrational spectroscopic characteristics of the Cu-ZnO between 4000 and 400 cm^{-1}. The structural study was captured using Cu-K radiation (λ = 1.54Å) at 40 kV using a Bruker AXS model D8 Advance diffractometer. A JEOL 6390 LA Scanning Electron Microscope was used to examine the surface morphologies of the samples. Specifically, the UV-DRS spectra of the Cu-ZnO in DMSO solution was recorded between 200 and 900 nm using a PERKIN ELMER spectrometer. The JASCO FP-8300 PL spectrometer was used to acquire PL spectra at an excitation wavelength of 260 nm. The Metrohm Autolab M204 electrochemical workstation was used to take the readings, and it had a standard three-electrode arrangement for the measurements.

3. Result and discussion

3.1. Vibrational and crystallinity studies

In order to identify the most prominent functional group in the catalyst, FTIR measurements were conducted at room temperature. The FTIR spectrum (Fig.1) shows Cu-ZnO nanoparticles. FTIR peaks at 501 cm^{-1} are attributable to stretching vibrations in the metal-oxygen bond. Peak broadness is indicative of the crystalline character of Cu-ZnO NPs. The symmetric and asymmetric stretching mode vibrations of the CO_2 molecule in air created the absorption band at 2428.06 cm^{-1} [17]. The catalyst's surface may have absorbed stretching and bending vibrations of the OH group from the surrounding environment, which might account for the broad peak at 3461.77, 1384.71, and 1637cm^{-1} [18].

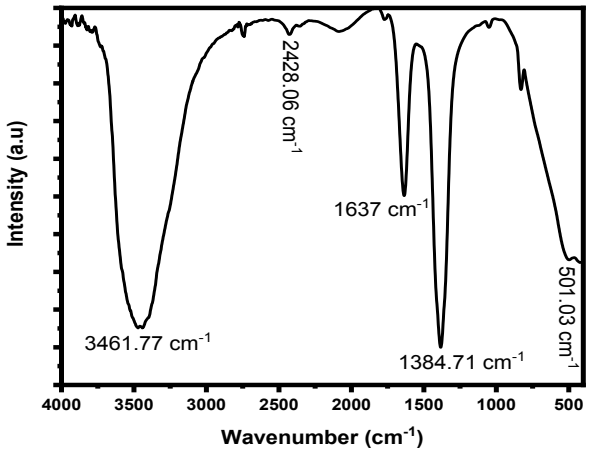

Fig. 1. FTIR spectra of Cu-ZnO prepared by the green synthesis using maize

PXRD is an essential technique for characterizing nanostructures and other small-scale samples by elucidating their structure, elemental composition, elemental phase, and elemental type. PXRD data may also be used to estimate the crystallite size of a given sample. PXRD data for as-prepared Cu-ZnO NPs, recorded at 2θ values from 10^{o} to 70^{o}, is shown in Fig.2.

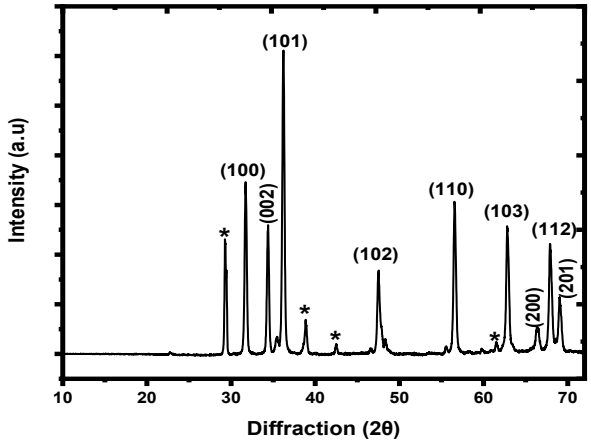

Fig. 2. Diffraction pattern of Cu-ZnO prepared by the green synthesis using maize

From the PXRD pattern, well-defined diffraction peaks clearly demonstrate the crystalline nature, with peaks corresponding to the angle 2θ and planes of 31.7° (100), 34.4° (002), 36.2° (101), 47.5° (102), 56.5° (110), 62.8° (103), 66.5° (200), 67.9° (112) and 69° (201), indicating the hexagonal structure wurtzite ZnO. The addition of dopant reduces constantly the intensities recorded at peaks (100) and ((002)[19]. The occurrence of additional peaks at 2θ = 29.2° (110), 42.4° (200), and 61.5° (220) of cubic copper phase (JCPD no. 77-0199)[20]. After measuring the Cu-ZnO crystals as-prepared, the crystallite (average) size was found to be 23.5nm using conventional Scherrer formula[21].

$$D = \frac{K\lambda}{\beta cos\theta} \tag{1}$$

where D - crystallite size(avg.), λ- radiation wavelength of the incoming light (in this case, Cu Kα with a wavelength of 1.540Å), K is a constant (0.89), often known as the shape factor, β - FWHM, and θ is the diffraction angle.

3.2. Morphology and elemental studies

The surface morphology of nanoscale materials is a crucial feature that must be considered before using such nanomaterials in a variety of applications. Fig.3 displays the surface morphology and elemental analysis of Cu-ZnO nanoparticles. The exterior surface morphology of Cu-ZnO nanoparticles demonstrates that the agglomerated Cu-ZnO nanoparticles have fashioned the particles into spherical shapes. In Fig. 3a, FESEM micrographs reveal Cu-ZnO nanoparticles that have grown in size and become highly agglomerated. These microparticles are produced when nanoparticles agglomerate into larger particles[22]. The Cu inclusion in ZnO nanoparticles may have reduced particle size and aggregation, which matches XRD crystallite size. The EDX spectra were used to record the elemental analysis of Cu-ZnO, and the results demonstrate the existence of copper in addition to zinc and oxygen[20].

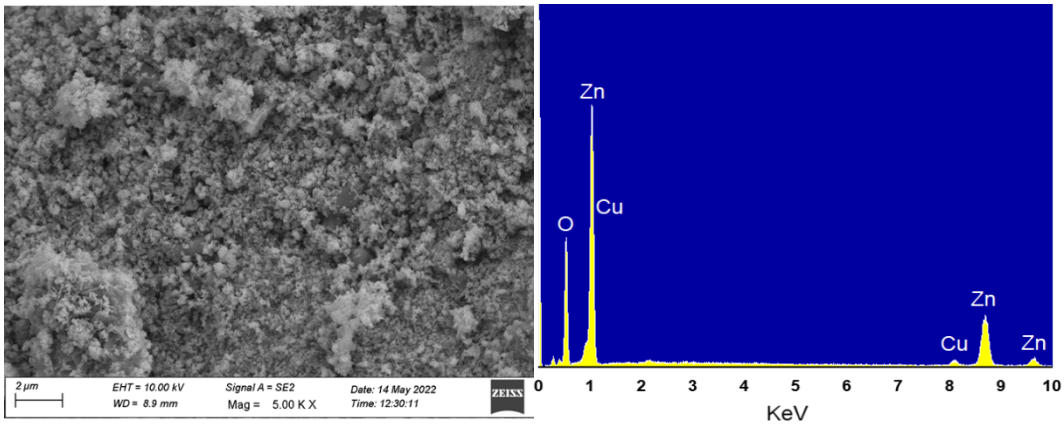

Fig. 3. SEM and EDS spectra of Cu-ZnO prepared by the green synthesis using maize

3.3. Optical studies

The primary motivation behind doping is to significantly boost visible-range solar energy absorption. The spectra of absorption were recorded (200-800nm) to investigate the optical characteristics of doped ZnO. As can be seen in Fig.4(left), λ_{max} (λ corresponding to peak) for pure ZnO is 368 nm. Doping raises λ_{max} to its maximum value of 371 nm as a result of the incorporation of a negligible amount of Cu[23]. The optical band gap of the produced materials was evaluated using Tauc's equation[24].

$$[F(R)h\upsilon/t]^{1/n} = A\,(h\upsilon - E_g) \tag{2}$$

where 'F(R) = (1 R)^2/2R)'- Kubelka–Munk function, 't'- thickness of the material, R- reflectance spectrum, n-band gap transition, A- constant of proportionality, and h - energy of photon. Fig.4(right) depicts Tauc's plot between the relationship h and [F (R)h]^2 and the tangent line drawn to meet the x-axis line (B). Based on the figure, the energy band gap (E_g) for Cu-ZnO was calculated to be 3.07 eV.

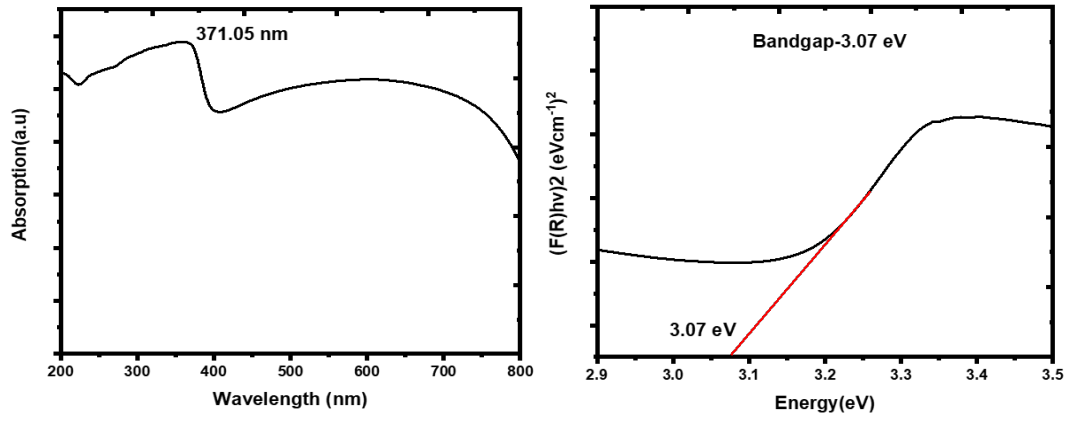

Fig. 4. Absorption and bandgap spectra of Cu-ZnO prepared by the green synthesis using maize

In view to examine the optical characteristics, then impacts of ZnO loaded Cu in a photoluminescence investigation was performed at room temperature. Photoluminescence of Cu-doped zinc oxide is shown in Fig. 5. An excitonic peak can be seen in the ultraviolet area of all of the spectra, and a defect-associated peak can be seen in the visible range. This peak is mostly attributable to ZnO defects. Every one of them has an ultraviolet emission peak close to 397 nm.

Near band-edge (NBE) emission, which is associated with this ultraviolet spectrum, is mostly associated with the recombination of free excitations[25]. Furthermore, the spectra exhibit modest blue-green emission peaks at around 464.5 nm[26].

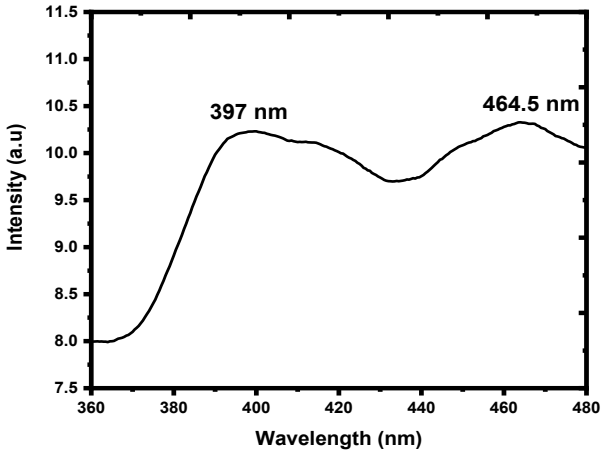

Fig. 5. PL spectra of Cu-ZnO prepared by the green synthesis using maize

3.4. Cyclic voltametric studies

Cyclic voltammetry (CV) in KOH (1M) solution was used to observe electrochemical characteristics of electrodes coated with Cu-ZnO nanoparticles. The standard three-electrode system seen in electrochemical workstations consists of a working electrode (Glassy carbon), a electrode of counter (Pt wire), and a electrode of reference (Silver-silver chloride). Using a scan rate of 10-100 mVs^{-1}, Fig. 6 displays the CV curves of Cu-ZnO nanoparticle coated electrodes across a range of potential 0.1 to 0.6 V. Cyclic-voltametric curves demonstrate the oxidation peak of Zn^{2+} and Zn^{3+} in the anodized and reduction peaks of 0.1 to 0.6 V in the cathodic area, with the redox peak shifting as rate of scanning increased on or after 10-100 mV/s. More importantly, linear rise in redox current peaks with an increasing scan rate hints to the process in charge transfer at the interface owing to redox effects and a rapid increase in the rate of mobility in electrons and ions[27]. Based on these results, it's obvious that the pseudo-capacitive properties of Cu-ZnO originate from the faradic efficiency of the particles in the electrolytic solution and the loads on the surface of the working materials.

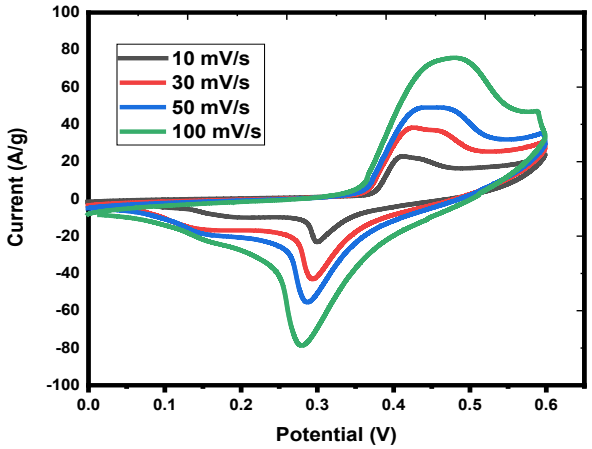

Fig. 6. CV studies of Cu-ZnO prepared by the green synthesis using maize

Improved intercalation between the carrier particles in the electrolyte and the working electrode is reflected in increased pseudo-capacitive activity in Cu-ZnO, which can be traced back to the formation of a standardized and full nanosphere structure shown in SEM images[28].

4. Conclusion

Here, we show that natural extracts from maize waste materials may serve as an efficient reducing, stabilizing, and chelating agent during the production of crystalline copper-loaded zinc oxide nanoparticles, making this method green, unique, and environmentally friendly. The Cu loaded ZnO nanoparticles are biosynthesized with the help of phytochemicals contained in the extracts of waste maize material. XRD (X-ray diffraction) was employed to evaluate structure and phase of Cu-ZnO, confirming that the Zinc oxide nanoparticles had a hexagonal structure. Crystallite size dispersion of Cu-ZnO nanoparticles has been measured and found to be 23.5 nm. PL and UV-Vis techniques were employed to investigate optical properties of Cu-ZnO nanoparticles. Incorporating Cu into ZnO reduces surface imperfections such oxygen vacancies and zinc vacancies, as shown by the photoluminescence analysis. The functional groups of Cu-ZnO were detected between 600 and 400 cm^{-1}, so validating the presence of Cu and Zn oxides. Through the use of FESEM, the surface morphology of Cu-ZnO nanoparticles was documented, and it was found to be round in shape. As a result, the Cu loading altered the band gap of ZnO, which is significant for photocatalysis and solar cells equipment. In the future, the cost efficacy of produced metal oxides will be determined in contrast to standard synthesis techniques.

References

[1] Sun, Y., Chen, G., Xi, S., Xu, Z.J., ACS Catalysis. 11, 13947-13954 (2021); https://doi.org/10.1021/acscatal.1c04393

[2] Haider, A., Ikram, M., Rafiq, A.,Green Nanomaterials as Potential Antimicrobials. pp. 25-46. Springer (2023); https://doi.org/10.1007/978-3-031-18720-9_2

[3] Benrezgua, E., Deghfel, B., Abdelhalim, Z., Basirun, W.J., Amari, R., Boukhari, A., Yaakob, M.K., Kheawhom, S., Mohamad, A.A., Journal of Molecular Structure. 133639 (2022); https://doi.org/10.1016/j.molstruc.2022.133639

[4] Arya, S., Mahajan, P., Mahajan, S., Khosla, A., Datt, R., Gupta, V., Young, S.-J., Oruganti, S.K., ECS Journal of Solid State Science and Technology. 10, 023002 (2021); https://doi.org/10.1149/2162-8777/abe095

[5] Benabdellah, A.C., Zekhnini, K., Cherrafi, A., Garza-Reyes, J.A., Kumar, A., Business Strategy and the Environment. 30, 4037-4053 (2021); https://doi.org/10.1002/bse.2855

[6] Kaur, I., Priya, N., Kumari, A., Chaudhary, V., Batra, V., ECS Transactions. 107, 19443 (2022); https://doi.org/10.1149/10701.19443ecst

[7] Shamaila, S., Sajjad, A.K.L., Farooqi, S.A., Jabeen, N., Majeed, S., Farooq, I., Applied Materials Today. 5, 150-199 (2016); https://doi.org/10.1016/j.apmt.2016.09.009

[8] García-Lara, S., Serna-Saldivar, S.O., Corn. 1-18 (2019); https://doi.org/10.1016/B978-0-12-811971-6.00001-2

[9] Hussain, S., Ijaz, M., Hussain, M., Ul-Allah, S., Abbas, T., Nawaz, A., Nawaz, M., Ahmad, S., Agronomic crops. pp. 237-260. Springer (2019); https://doi.org/10.1007/978-981-32-9151-5_13

[10] Wang, K.-J., Zhao, J.-L., Biomedicine & Pharmacotherapy. 110, 510-517 (2019); https://doi.org/10.1016/j.biopha.2018.11.126

[11] Lv, Z., Sun, H., Du, W., Li, R., Mao, H., Kopittke, P.M., Science of The Total Environment. 796, 148927 (2021); https://doi.org/10.1016/j.scitotenv.2021.148927

[12] Adebisi, J.A., Agunsoye, J.O., Bello, S.A., Haris, M., Ramakokovhu, M.M., Daramola, M.O., Hassan, S.B., Particulate Science and Technology. 38, 667-675 (2020); https://doi.org/10.1080/02726351.2019.1578845

[13] Dağhan, H., Applied Ecology and Environmental Research. 16, (2018).
[14] Roy, D., Adhikari, S., Adhikari, A., Ghosh, S., Azahar, I., Basuli, D., Hossain, Z., Chemosphere. 287, 131911 (2022); https://doi.org/10.1016/j.chemosphere.2021.131911
[15] Tong, X., Guo, N., Dang, Z., Ren, Q., Shen, H., Iet Nanobiotechnology. 12, 987-993 (2018); https://doi.org/10.1049/iet-nbt.2017.0230
[16] Del Buono, D., Di Michele, A., Costantino, F., Trevisan, M., Lucini, L., Nanomaterials. 11, 1270 (2021); https://doi.org/10.3390/nano11051270
[17] Boudiaf, M., Messai, Y., Bentouhami, E., Schmutz, M., Blanck, C., Ruhlmann, L., Bezzi, H., Tairi, L., Mekki, D.E., Journal of Physics and Chemistry of Solids. 153, 110020 (2021); https://doi.org/10.1016/j.jpcs.2021.110020
[18] Sharma, P.K., Singh, M.K., Sharma, G.D., Agrawal, A., Materials Today: Proceedings. 43, 3061-3065 (2021); https://doi.org/10.1016/j.matpr.2021.01.400
[19] Byrne, C., Moran, L., Hermosilla, D., Merayo, N., Blanco, Á., Rhatigan, S., Hinder, S., Ganguly, P., Nolan, M., Pillai, S.C., Applied Catalysis B: Environmental. 246, 266-276 (2019); https://doi.org/10.1016/j.apcatb.2019.01.058
[20] Ben Saad, L., Soltane, L., Sediri, F., Russian Journal of Physical Chemistry A. 93, 2782-2788 (2019); https://doi.org/10.1134/S0036024419130259
[21] Chen, F., Zhang, P., Xiao, L., Liang, J., Zhang, B., Zhao, H., Kosol, R., Ma, Q., Chen, J., Peng, X., ACS Applied Materials & Interfaces. 13, 8191-8205 (2021); https://doi.org/10.1021/acsami.0c18600
[22] Alhajj, N., Zakaria, Z., Naharudin, I., Ahsan, F., Li, W., Wong, T.W., Asian journal of pharmaceutical sciences. 15, 374-384 (2020); https://doi.org/10.1016/j.ajps.2019.02.001
[23] Sanakousar, F.M., Vidyasagar, C., Jiménez-Pérez, V.M., Prakash, K., Materials Science in Semiconductor Processing. 140, 106390 (2022); https://doi.org/10.1016/j.mssp.2021.106390
[24] Kaya, D., Aydınoğlu, H.S., Tüzemen, E.Ş., Ekicibil, A., Thin Solid Films. 732, 138800 (2021); https://doi.org/10.1016/j.tsf.2021.138800
[25] Jalolov, R.R., Urolov, S.Z., Shaymardanov, Z.S., Kurbanov, S.S., Rustamova, B.N., Materials Science in Semiconductor Processing. 128, 105783 (2021); https://doi.org/10.1016/j.mssp.2021.105783
[26] Borade, P.A., Sant, T., Gokarna, A., Joshi, K.U., Panat, R.P., Jejurikar, S.M., Optical Materials. 109, 110348 (2020); https://doi.org/10.1016/j.optmat.2020.110348
[27] Dhiman, P., Kumar, A., Shekh, M., Sharma, G., Rana, G., Vo, D.-V.N., AlMasoud, N., Naushad, M., ALOthman, Z.A., Environmental research. 197, 111074 (2021); https://doi.org/10.1016/j.envres.2021.111074
[28] Xue, Y., Zheng, S., Xue, H., Pang, H., Journal of Materials Chemistry A. 7, 7301-7327 (2019); https://doi.org/10.1039/C8TA12178H